Chem. Pap. (2017) 71:2301–2308
DOI 10.1007/s11696-017-0224-6

ORIGINAL PAPER

Development of a fast, simple, and sensitive colorimetric method to determine benzothiazole based on the plasmonic response of gold nanoparticles

Raziyeh Asrariyan[1,2] · **Shahla Elhami**[1,2]

Received: 16 March 2017 / Accepted: 3 June 2017 / Published online: 24 June 2017

Abstract In this article, for the first time, benzothiazole (BT) was determined using a simple, fast, and sensitive colorimetric method. This method was based on the surface plasmon resonance (SPR) property of gold nanoparticles (AuNPs) and interaction between BT and gold nanoparticles. The addition of BT leads to AuNPs aggregation with red-to-blue color shifts. TEM analysis demonstrated aggregation of gold nanoparticles at the presence of BT. The effective parameters in the SPR such as solution pH, concentration of AuNPs, standing time, electrolyte concentration, and coexisting substances were studied and optimized. Under the optimum conditions, this method exhibited a linear range from 10 to 200 ng mL^{-1} ($R^2 = 0.996$), with a detection limit of 1 ng mL^{-1}. Relative standard deviations (RSD) for 40.0 and 140.0 ng mL^{-1} of BT were 2.5 and 1.5%, respectively. Possible mechanism for the SPR changes of AuNPs in the presence of BT was discussed. Moreover, the cost-effective colorimetric method has successfully been applied for the analysis of various real samples.

Keywords Benzothiazole · Colorimetric method · Gold nanoparticle · Surface plasmon resonance

Introduction

Benzothiazole (BT) is used in a variety of industrial processes, so it is produced in high volumes (Avagyan et al. 2013, 2015). BT has been produced in the range of 4.5–450 tons in the US (Asimakopoulos et al. 2013). BT is a prototype for benzothiazole derivatives (BTs). BTs have a wide range of applications; for example, they are used as vulcanization accelerators in rubber production, corrosion inhibitors in antifreeze, photo sensitizers in photography, slimicides in the paper and pulp industry, fungicides in lumber and leather industries, biocides, and constituents of azo dyes (Avagyan et al. 2013, 2015; Asimakopoulos et al. 2013; Domínguez et al. 2012; Speltini et al. 2016; Fries 2011). BTs are used in the production of drugs, de-icing/anti-icing fluids, and food flavors. Owing to a wide range of applications for BT, there are so many sources to pollute water, soil, and environmental samples (Fries 2011). BT has been measured in wastewater (i.e., domestic and industrial), surface water (i.e., river and lake) (Domínguez et al. 2012), and soil (Speltini et al. 2016). BTs have negative effects on aquatic organisms and mammals even at low concentrations; therefore, they are important pollutants for the environment (Xu et al. 2015). They have been known as dermal sensitizers, respiratory tract irritants, and carcinogenic in humans (Asimakopoulos et al. 2013; Herrero et al. 2014a, b). The methods to measure benzothiazole have been reported in several articles (Xu et al. 2015; Herrero et al. 2014a, b; van Leerdam et al. 2009; Naccarato et al. 2014; Silva et al. 2014; Kloepfer et al. 2004). Liquid chromatography (LC) and gas chromatography (GC) coupled with mass spectrometry are the preferred instrumental analytical techniques. Some of these methods are laborious and require sophisticated instruments. To the best of our knowledge, there has not been any report on the

✉ Shahla Elhami
sh.elhami@iauahvaz.ac.ir

[1] Department of Chemistry, Khouzestan Science and Research Branch, Islamic Azad University, Ahvaz, Iran

[2] Department of Chemistry, Ahvaz Branch, Islamic Azad University, Ahvaz, Iran

determination of BT using the spectrophotometric method. Spectrophotometric methods are attractive alternatives in consequence of advantages such as the instrumentation common availability, simple operation, low cost, high speed, precision, and accuracy of the technique.

In the last decade, gold nanoparticles have attracted the attention due to their special properties. AuNPs are prepared by chemical reduction of gold salts in the presence of an appropriate stabilizer which binds to their surface to impart high stability and prevent particle aggregation. Several reducing and stabilizing agents were used that citrate is the most popular one (Guo and Wang 2007; Ghosh et al. 2008). AuNPs are suited for different applications due to their various and especial properties such as optical, electronic, magnetic, and catalytic properties (Dumur et al. 2011). One of the interesting properties of gold nanoparticles is surface plasmon resonance (SPR) which gives them a specific optical behaviour. Due to SPR properties, when the nanoparticles aggregate, the red color of gold nanoparticle solutions turns to blue. Gold nanoparticles are widely used to determine of metal cations (Thatai et al. 2016; Huang et al. 2016) and organic compounds (Khodaveisi et al. 2017) by spectrophotometric method.

Hereon, a safe, simple, and sensitive method to determine BT was established based on SPR property of gold nanoparticles.

Experimental

Chemical and substances used

The chemicals of analytical grade were used throughout this study without further purification. All chemicals were purchased from Merck (Merck, Darmstadt, Germany) and double distilled water was used throughout. A stock solution of 1000 mg L^{-1} of benzothiazole was prepared by dissolving 0.100 g of the benzothiazole in acetone and diluting to 100 mL in a volumetric flask. More diluted solutions were prepared daily using this stock solution.

Absorption studies were carried out using a UV–Vis spectrophotometer model Genesis10s (Miltonroy, American). The pH was measured using an Inolab wtw720 (Germany). Transmission electron microscopy (TEM) images AuNPs were recorded using a Zeiss-EM10C-100 kV (Germany).

Preparation of gold nanoparticle

For synthesizing the gold nanoparticles, trisodium citrate was used as the reducing agent (Alkilany et al. 2016). First, 100 mL of 0.25 mM $HAuCl_4$ solution was heated to boiling. Then, 3 mL of a 1% trisodium citrate solution was added quickly to the solution. After 5 min at the same temperature, the color of solution changed from light yellow to gray, and finally became deep red. After the color change, the reaction continued for an additional 5 min, and then, the heater was turned off and the solution was stirred until it reached the room temperature. The solution was stored at 4 °C.

General procedure

In this procedure, 2 mL prepared AuNPs solution (0.25 mM), 1 mL of formate buffer (pH 3.5), and different concentrations of benzothiazole were added to 10 mL volumetric flasks and diluted with double distilled water. The solution was shaken and a portion was transferred to a 1 cm spectrophotometric cell to record absorbance spectrum. The same procedure was done on blank without the presence of benzothiazole.

Sampling

To prepare the tire rubber sample, at first, a piece of tire rubber was cut and the sample was produced by abrading the tire rubber using stainless coarse emery. Portions of around 1.0 g of tire rubber particles were placed in test tubes and 10 mL acetone in dichloromethane (20%) was added. The test tubes were placed in an ultra-sonication bath for 1 h. Then, the samples were filtered and the extraction was repeated with fresh solvent. 2.0 mL distilled water was added to the samples to avoid volatilization of BT during solvent evaporation. The solution was evaporated to a small volume (about 5 mL). Afterward, the solution was transferred to a 25 mL volumetric flask and diluted with methanol (Avagyan et al. 2013). 0.5 mL of this solution was treated under the general procedure.

The extraction of BT from urban roadside soil sample (collected from Pasdaran Street in Ahvaz, Iran) was carried out according to the following procedure (Speltini et al. 2016). The soil sample (3.0 g) was placed in test tubes and 6 mL methanol was added and was heated (for 10 min). The cooled suspension was centrifuged for 10 min at 4500 rpm. The recovered supernatant solution was transferred to a 25 mL volumetric flask and diluted with methanol–water (1:1).

The water samples were chosen from various sources (domestic wastewater, Karoon River, and Ahvaz tap water samples). The collected water samples were filtered using a filter paper (Whatman No. 40) to eliminate impurities and suspended solids, and then, they were acidified with HNO_3 prior to use. An aliquot of water samples was treated under the recommended procedure.

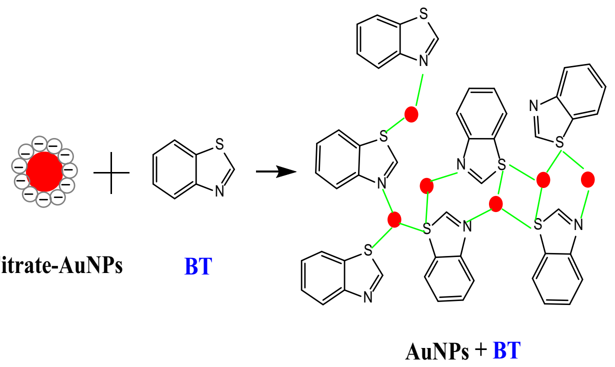

Scheme 1 Suggested mechanism for the interaction between gold nanoparticles and BT molecules

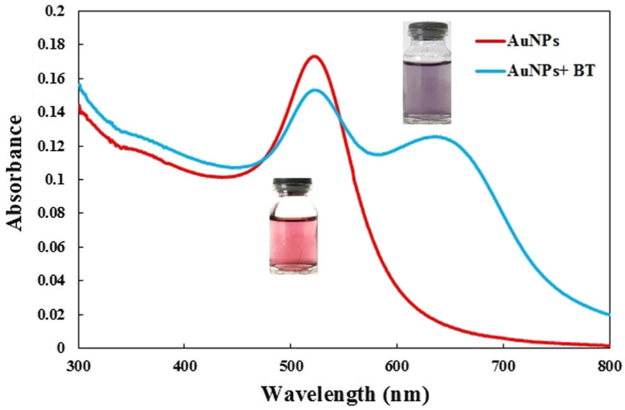

Fig. 1 UV–Vis spectra of AuNPs in the absence (*red*) and presence of BT (*blue*)

Results and discussion

UV–Vis absorption spectroscopy is a widely used technique in the characterization of the optical properties of AuNPs, because the position and the intensity of the surface plasmon band of colloidal gold are related to the shape and the size of gold nanoparticles (Venditta et al. 2015).

It is well known that the peak wavelength, $\lambda_{\max}$, and intensity of the SPR spectrum are dependent upon the size, shape, and interparticle spacing of the nanoparticle. Owing to the changes of SPR properties, the red color of gold nanoparticle solutions turns to blue when the nanoparticles aggregate (Lai et al. 2017; Hormozi Nezhad et al. 2008). In the presence of substances with groups S or N, AuNPs are aggregated and the color of the solution changes to blue (Deng et al. 2014; Kumar et al. 2003; Parham et al. 2015; Farkhari et al. 2016). Accordingly, BT is capable of aggregating AuNPs. BT could connect the AuNPs together to make the aggregation. Scheme 1 shows the formation of BT–AuNPs aggregations. The aggregation of AuNPs led to a change in color from wine-red to blue–purple (Fig. 1).

TEM analysis

The structural characteristics such as shape and size of AuNPs and AuNPs–BT and also aggregation phenomenon were investigated by TEM analysis (Fig. 2). The nanoparticles are almost spherical. The size of AuNPs according to the TEM image (Fig. 2a) was approximately about 12–15 nm. Upon the addition of BT, AuNPs aggregated due to the presence of substance with groups S and N (Fig. 2b).

Optimization of experimental conditions

Effect of pH

Solution pH is a crucial factor to determine BT in this method. Therefore, the effect of pH on the absorbance of the system was studied over a pH range of 3–6. The dilute HCl and NaOH solutions were used to adjust the pH of the solutions. As can be seen from Fig. 3, the absorbance ratio is maxima in pH $= 3.5$. It is well known that AuNPs are negatively charged (Deng et al. 2014; Kumar et al. 2003); therefore, it is reasonable that the connection between

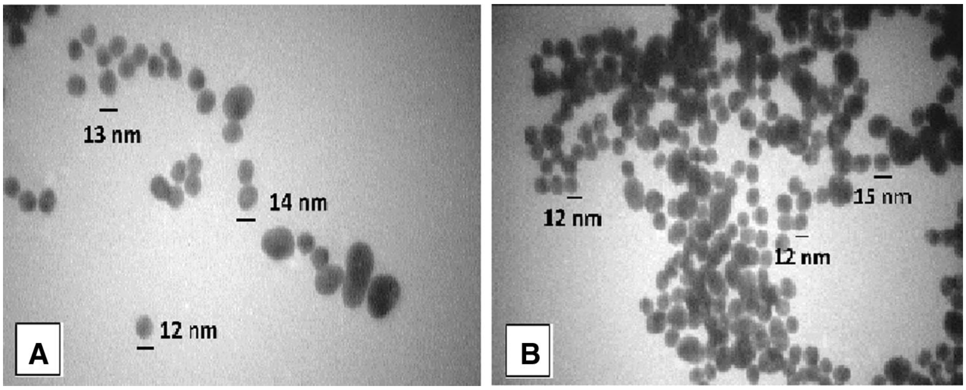

Fig. 2 TEM of AuNPs before and after addition of BT: **a** TEM of AuNPs and **b** TEM of AuNPs–BT

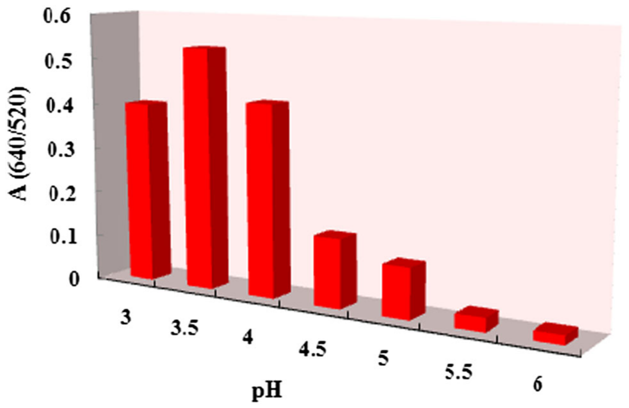

Fig. 3 Influence of pH on the surface plasmon intensity; the pH of test solution was adjusted with dilute NaOH or HNO_3 (experimental condition: aqueous sample volume, 10 mL; AuNPs concentration, 50 µmol L^{-1}; [BT] = 100 ng mL^{-1})

AuNPs and BT occurs at a lower pH as a consequence of AuNPs neutralization.

To choose the optimal buffer, three buffers (i.e., formate, phthalate, and oxalate buffer) were investigated that formate buffer was the best (Fig. 4), because using 0.8–1.2 mL of formate buffer was created the necessary conditions. Furthermore, 1.0 mL of formate buffer was selected as optimum.

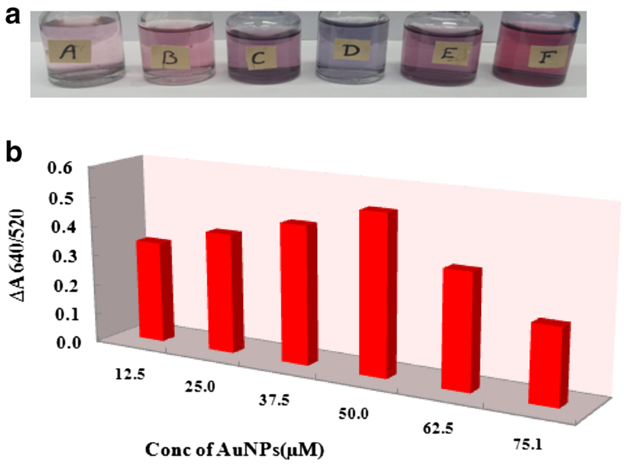

Fig. 5 **a** Photographs of solution *A*: 12.5, *B*: 25.0, *C*: 37.5, *D*: 50.0, *E*: 62.5, and *F*: 75.1 µM AuNPs; **b** influence of AuNPs concentration on the surface plasmon intensity (experimental condition: aqueous sample volume, 10 mL; BT concentration, 100 ng mL^{-1}, volume of formate buffer, 1 mL)

Effect of AuNPs concentration

The AuNPs concentration has an important role in the sensitivity of the method. In this section, different amounts of AuNPs solution were used to study the absorption spectra. According to Fig. 5a, the most change in color was shown for solution D. As shown in Fig. 5b, A640/A520 ratio increased by enhancing the amount of AuNPs, the solution D (AuNPs concentration: 50 µM) had maximum absorbance ratio, and then by increasing the amount of AuNPs, absorbance ratio decreased. Therefore, 50.0 µM of AuNPs concentration was selected as the optimum amount. As a consequence, the aggregations of AuNPs can be better when AuNPs and BT exist in solution with suitable ratio; if one of them is present in excess, aggregations will be destroyed.

Effect of interaction time

The effect of interaction time on absorption spectra was investigated in the range of 1–10 min. In the all cases, the absorption spectra did not vary significantly. This means that the interaction of BT and AuNPs does not require time and is very fast.

Effect of electrolyte

High concentrations of electrolytes usually affect SPR processes. To study the electrolyte effect, the experiments

Fig. 4 Influence of buffer on the surface plasmon intensity (experimental condition: aqueous sample volume, 10 mL; AuNPs concentration, 50 µmol L^{-1}; [BT] = 100 ng mL^{-1})

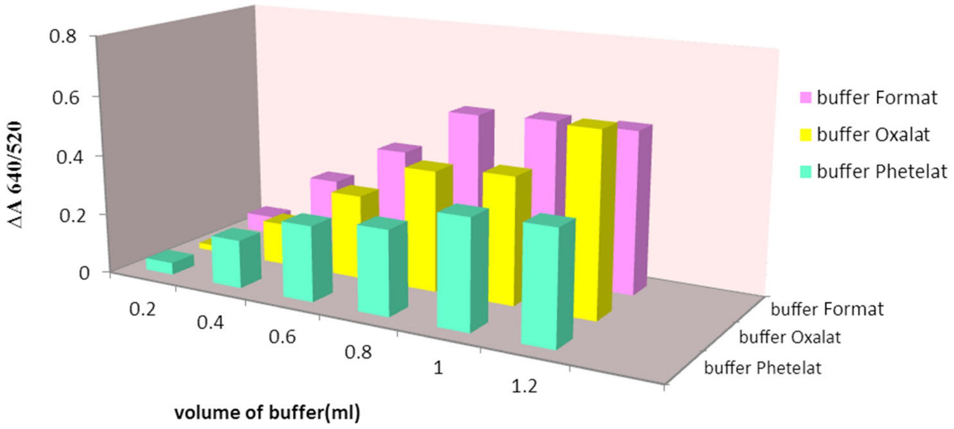

were carried out by adding different salts such as NaCl, KCl, and Na_2CO_3. The results in Fig. 6 indicate that the addition of up to 10 mM of NaCl, KCl, and 5 mM of Na_2CO_3 did not have any significant effects on the A640/A520 ratio. In the high concentration of electrolytes, it was observed that the color of the sample solution is close to the color of blank solution and the A640/A520 ratio was decreased. However, it is possible that electrolytes could change the surface of nanoparticles (Parham et al. 2015; Farkhari et al. 2016), so that in the high concentration of electrolytes, interaction between BT and nanoparticles decreased and thus aggregation decreased.

Analytical features of the method

A linear calibration graph was drawn for the determination of BT under the proposed experimental conditions. The

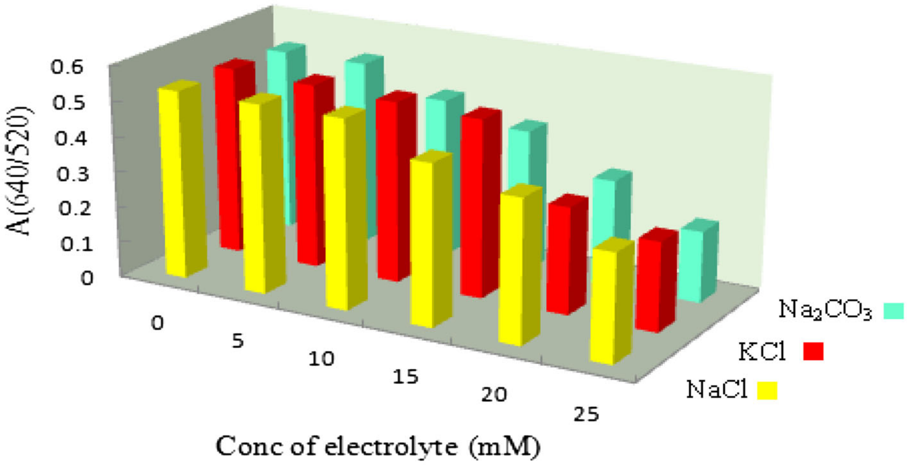

Fig. 6 Influence of electrolyte on the surface plasmon intensity (experimental condition: aqueous sample volume, 10 mL; AuNPs concentration, 50 µmol L^{-1}; BT concentration, 100 ng mL^{-1}, volume of formate buffer, 1 mL)

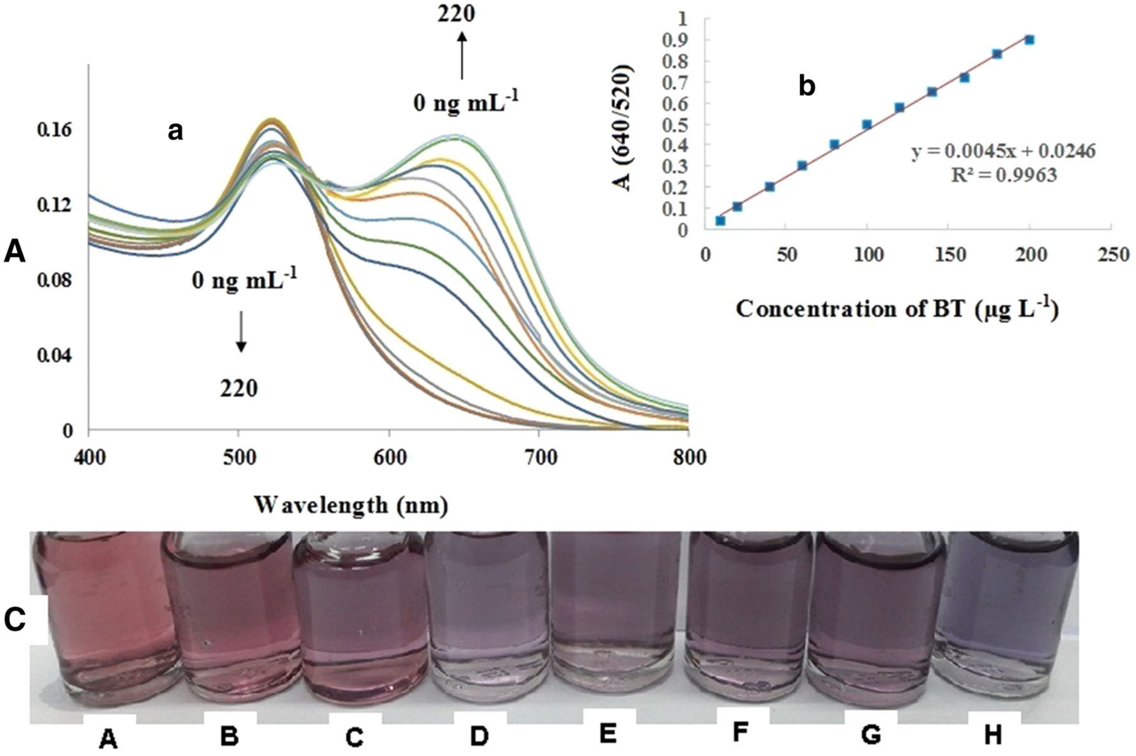

Fig. 7 Overlaid UV–Vis spectra of AuNPs–BT and calibration graph for determination of BT. **a** Overlaid UV–Vis spectra of AuNPs–BT from 0 to 220 ng mL^{-1} BT. **b** Calibration graph from 10 to 200 ng mL^{-1} BT. **c** Photographs of solution *A*: 10.0, *B*: 40.0, *C*: 80.0, *D*: 100.0, *E*: 140.0, *F*: 160.0, *G*: 180.0, and *H*: 200.0 ng mL^{-1} BT (experimental condition: aqueous sample volume, 10 mL; AuNPs concentration, 50 µmol L^{-1}; volume of formate buffer, 1 mL)

Table 1 Concentration and tolerance limit of foreign ions on determination of BT

Interference	Concentration of interfering ion (μg mL^{-1})	Tolerance limits [*X*]/BT
Na^+, Cl^-, K^+, SO_4^{2-}, CO_3^{2-}, NO_3^-, Cu^{2+}, Mn^{2+}, NH_4^+, SO_3^{2-}	100	1000
Ni^{2+}, Fe^{3+}	30	300
Zn^{2+}, Ba^{2+}	20	200
Bi^{3+}	10	100
Ca^{2+}, Co^{2+}	5	50
Mg^{3+}, Fe^{2+},Cd^{2+}, Al^{3+}	2	20

method showed good linearity over the calibration range 10–200 ng mL^{-1} (Fig. 7). The correlation of determination (r^2) was 0.996. The detection limit of BT was determined to be 1 ng mL^{-1} which was calculated using the formula $3S_b$/slope, where S_b represents the standard deviation of the blank and slope is obtained from the linear calibration graph. The results obtained clearly indicate that this method can be potentially used to detect BT with high sensitivity. The relative standard deviations (RSD) for ten replicate measurements of 40 and 140 ng mL^{-1} of BT were 2.5 and 1.5%, respectively.

Effect of interfering ions

The possible interference of other cations and anions on the detection of BT was investigated. Interference studies were performed by spiking various ions to the solutions containing 100 ng mL^{-1} of BT and applying the general procedure. The tolerance limit was defined as the maximum concentration of potentially interfering ions causing ±5% error in the determination of BT. The results in Table 1 indicate that the developed method is relatively selective for the determination of BT.

Analysis of real sample

To assess the applicability of the method, it was applied to the determination of BT in tap water, river water, domestic wastewater, industrial wastewater, urban roadside soil, and tire rubber samples. To estimate the influence of the matrix, all the samples were spiked with different concentrations of BT in the linear range to determine the recovery, and then, a general method at optimum conditions was performed. These results (Table 2) indicated that the proposed method was helpful for the determination of BT not only in water samples but also in complex matrixes such as soil and tire rubber.

Table 2 Determination of BT in real samples

Sample	Added BT (ng mL^{-1})	Founded[a] BT (ng mL^{-1})	Recovery (%)
Tap water	0	ND	–
	60	62.1 ± 0.1	103.5
	100	102.2 ± 0.2	102.2
River water	0	ND	–
	50	48.2 ± 0.2	96.4
	100	97.8 ± 0.3	97.8
Domestic wastewater	0	75.0 ± 0.2	–
	20	95.8 ± 0.3	104.0
	50	122.9 ± 0.3	95.8
Industrial wastewater	0	30.2 ± 0.1	–
	20	49.3 ± 0.2	95.5
	50	82.1 ± 0.2	103.8
Urban roadside soil	0	ND	–
	30	28.8 ± 0.1	96.0
	100	102.5 ± 0.3	102.5
Tire rubber	0	79.8 ± 0.2	–
	50	130.4 ± 0.3	101.2
	70	147.5 ± 0.3	96.7

ND not detected

[a] Mean ± standard deviation ($n = 4$)

Conclusions

An AuNP-based colorimetric method for fast and sensitive detection of BT was developed and successfully applied for its determination in water, wastewater, tire, and urban roadside soil samples. This method based on the SPR property of AuNPs and the aggregation of AuNPs at the presence of BT, therefore, caused a visible color change from red to blue. TEM images showed the formation of aggregated particles of AuNPs–BT. The most important advantage of the proposed method is the possibility of BT determination with very good accuracy and sensitivity using a simple UV–Vis spectrometer and without any expensive or sophisticated instrumentation. A comparison between the proposed method and the previously published methods for BT determination is shown in Table 3. The dynamic range, detection limit, and RSD of the present method are close to or better than the reported methods.

Table 3 Comparison of the proposed method with some of the previously reported methods for the determination of BT

Number	Method	Linear range (ng mL^{-1})	Detection limit (ng mL^{-1})	RSD (%)	Real sample	References
1	Ionic liquid stationary phases in GC–MS	31–3000	NG	10	Wastewaters	Domínguez et al. (2012)
2	HPLC	500–10000	150	8	Soil samples	Speltini et al. (2016)
3	GC–MS	NG	0.256	9.8	Untreated wastewater	Fries (2011)
4	LC–high-resolution MS	10–500	5	13	Sewage sludge	Herrero et al. (2014a)
5	SPE and analyzed by LC–electrospray MS	0.01–1.0	0.003	11	Drinking and surface water	van Leerdam et al. (2009)
6	LC–high-resolution MS	25–500	10	4	Sewage sludge	Herrero et al. (2014b)
7	Spectrophotometry	10–200	1	2.2	River water, tap water, wastewaters, soil, and tire	This study

GC gas chromatography, *MS* mass spectrometry, *NG* not given, *HPLC* high-performance liquid chromatography, *LC* liquid chromatography, *SPE* solid-phase extraction

The versatility with regard to the test samples in the suggested method is unique when compared to the reported methods in Table 3.

Acknowledgements The authors wish to thank Ahvaz Branch, Islamic Azad University and Ahvaz Ramin Power Plant for supporting this study.

References

Alkilany M, Caravana A, Hamaly M, Lerner K, Thompson L (2016) Phase transfer of citrate stabilized gold nanoparticles using nonspecifically adsorbed polymers. J Colloid Interface Sci 461:39–44. doi:10.1016/j.jcis.2015.09.010

Asimakopoulos AG, Wang L, Thomaidis NS, Kannan K (2013) Benzotriazoles and benzothiazoles in human urine from several countries: a perspective on occurrence, biotransformation, and human exposure. Environ Int 59:274–281. doi:10.1016/j.envint.2013.06.007

Avagyan R, Sadiktsis I, Thorsén G, Östman C, Westerholm R (2013) Determination of benzothiazole and benzotriazole derivates in tire and clothing textile samples by high performance liquid chromatography–electrospray ionization tandem mass spectrometry. J Chromatogr A 1307:119–125. doi:10.1016/j.Chroma.2013.07.087

Avagyan R, Luongo G, Thorsén G, Östman C (2015) Benzothiazole, benzotriazole, and their derivates in clothing textiles—a potential source of environmental pollutants and human exposure. Environ Sci Pollut Res 22:5842–5849. doi:10.1007/s.11356-014-3691-0

Deng HH, Weng ShH, Huang ShH, Zhang LN, Liu AL, Lin XH, Chen W (2014) Colorimetric detection of sulfide based on target-induced shielding against the peroxidase-like activity of gold nanoparticles. Anal Chim Acta 852:218–222. doi:10.1016/j.aca.2014.09.023

Domínguez C, Reyes-Contreras C, Bayona JM (2012) Determination of benzothiazoles and benzotriazoles by using ionic liquid stationary phases in gas chromatography mass spectrometry. Application to their characterization in wastewaters. J Chromatogr A 1230:117–122. doi:10.1016/j.chroma.2012.01.054

Dumur F, Guerlin A, Dumas E, Bertin D, Didier Gigmes D, Mayer CR (2011) Controlled spontaneous generation of gold nanoparticles assisted by dual reducing and capping agents. Gold Bull 44:119–137. doi:10.1007/s13404-011-0018-5

Farkhari N, Abbasian S, Moshaii A, Nikkhah M (2016) Mechanism of adsorption of single and double stranded DNA on gold and silver nanoparticles: investigating some important parameters in biosensing applications. Colloids Surf B 148:657–664. doi:10.1016/j.colsurfb.2016.09.022

Fries E (2011) Determination of benzothiazole in untreated wastewater using polar-phase stir bar sorptive extraction and gas chromatography–mass spectrometry. Anal Chim Acta 689:65–68. doi:10.1016/j.aca.2011.01.015

Ghosh P, Han G, De M, Kyu Kim Ch, Rotello VM (2008) Gold nanoparticles in delivery applications. Adv Drug Deliv Rev 60:1307–1315. doi:10.1016/j.addr.2008.03.016

Guo Sh, Wang E (2007) Synthesis and electrochemical applications of gold nanoparticles. Anal Chim Acta 598:181–192. doi:10.1016/j.aca.2007.07.054

Herrero P, Borrull F, Marcé RM, Pocurull E (2014a) A pressurised hot water extraction and liquid chromatography–higher solution mass spectrometry method to determine polar benzotriazole, benzothiazole and benzenesulfonamide derivates in sewage sludge. J Chromatogr A 1355(2014):53–60. doi:10.1016/j.chroma.2014.05.086

Herrero P, Borrull F, Pocurull E, Marce RM (2014b) A quick, easy, cheap, effective, rugged and safe extraction method followed by liquid chromatography-(Orbitrap) high resolution mass spectrometry to determine benzotriazole, benzothiazole and benzenesulfonamide derivates in sewage sludge. J Chromatogr A 1339:34–41. doi:10.1016/j.chroma.2014.02.081

Hormozi Nezhad MR, Alimohammadi M, Tashkhourian J, Mehdi Razavian S (2008) Optical detection of phenolic compounds based on the surface plasmon resonance band of Au nanoparticles. Spectrochim Acta A 71:199–203. doi:10.1016/j.saa.2007.12.003

Huang P, Li J, Liu X, Wu F (2016) Colorimetric determination of aluminum(III) based on the aggregation of Schiff basefunctionalized gold nanoparticles. Microchim Acta 183:863–869. doi:10.1007/s00604-015-1734-y

Khodaveisi J, Dadfarnia Sh, Haji Shabani AM, Saberi D (2017) Colorimetric determination of nabumetone based on localized surface plasmon resonance of functionalized gold nanoparticles as a chemical sensor. Sens Actuators B 239:1300–1306. doi:10.1016/j.snb.2016.09.110

Kloepfer A, Jekel M, Reemtsma T (2004) Determination of benzothiazoles from complex aqueous samples by liquid chromatography–mass spectrometry following solid-phase extraction. J Chromatogr A 1058:81–88. doi:10.1016/j.chroma.2004.08.081

Kumar A, Mandal S, Selvakannan PR, Pasricha R, Mandale AB, Sastry M (2003) Investigation into the interaction between surface-bound alkylamines and gold nanoparticles. Langmuir 19:6277–6282. doi:10.1021/la034209c

Lai TS, Chang TC, Wang SC (2017) Gold nanoparticle-based colorimetric methods to determine protein contents in artificial urine using membrane micro-concentrators and mobile phone camera. Sens Actuators B 239:9–16. doi:10.1016/j.snb.2016.07.158

Naccarato A, Gionfriddo E, Sindona G, Tagarelli A (2014) Simultaneous determination of benzothiazoles, benzotriazoles and benzosulfonamides by solid phase microextraction-gas chromatography-triple quadrupole mass spectrometry in environmental aqueous matrices and human urine. J Chromatogr A 1338:164–173. doi:10.1016/j.chroma.2014.02.089

Parham H, Pourreza N, Marahel F (2015) Resonance Rayleigh scattering method for determination of 2-mercaptobenzothiazole using gold nanoparticles probe. Spectrochim Acta A 151:308–314. doi:10.1016/j.saa.2015.06.108

Silva ALR, Cimas A, Ribeiro da Silva MDMC (2014) Energetic study of benzothiazole and two methyl benzothiazole derivatives: calorimetric and computational approaches. J Chem Thermodyn 73:3–11. doi:10.1016/j.jct.2013.06.021

Speltini A, Sturini M, Maraschi F, Porta A, Profumo A (2016) Fast low-pressurized microwave-assisted extraction of benzotriazole, benzothiazole and benezenesulfonamide compounds from soil samples. Talanta 147:322–327. doi:10.1016/j.talanta.2015.09.074

Thatai Sh, Khurana P, Prasad S, Soni SK, Kumar D (2016) Trace colorimetric detection of Pb^{2+} using plasmonic gold nanoparticles and silica–gold nanocomposites. Microchem J 124:104–110. doi:10.1016/j.micro.2015.07.006

van Leerdam JA, Hogenboom AC, van der Kooi MME, de Voogt P (2009) Determination of polar 1H-benzotriazoles and benzothiazoles in water by solid-phase extraction and liquid chromatography LTQ FT Orbitrap mass spectrometry. Int J Mass Spectrom 282:99–107. doi:10.1016/j.ijms.2009.02.018

Venditti I, Hassanein TF, Fratoddi I, Fontana L, Battocchio C, Rinaldi F, Carafa M, Marianecci C, Diociaiuti M, Agostinelli E, Cametti C, Russo MV (2015) Bioconjugation of gold-polymer core–shell nanoparticles with bovine serum amine oxidase for biomedical applications. Colloid Surf B 134:314–321. doi:10.1016/j.colsurfb.2015.06.052

Xu W, Yan W, Licha T (2015) Simultaneous determination of trace benzotriazoles and benzothiazoles in water by large-volume injection/gas chromatography–mass spectrometry. J Chromatogr A 1422:270–276. doi:10.1016/j.chroma.2015.10.017